Supplementary information: Surface hopping molecular dynamics simulation of ultrafast methyl iodide photodissociation mapped by Coulomb explosion imaging

Yijue Ding,[a,*] Loren Greenman,[a] and Daniel Rolles[a]

[a] James R. Macdonald Laboratory, Department of Physics, Kansas State University, Manhattan, KS 66502, USA

[*]Corresponding author: yijueding@gmail.com

1. Interpolating and extrapolating the potential energy surfaces

The potential energy surfaces are interpolated using the tri-cubic spline interpolation scheme. Such a multivariate interpolation scheme is equivalent to sequential interpolations on each dimension, but is implemented in a streamlined approach. We briefly summarize the tri-cubic scheme here, and more details can be found in Ref. [1].

The interpolation is perfomed on a structured grid such that the data points can be represented by

$$\begin{aligned} X &= \{x_1,\ldots,x_i,x_{i+1},\ldots,x_M\},\\ Y &= \{y_1,\ldots,y_j,y_{j+1},\ldots,y_N\},\\ Z &= \{z_1,\ldots,z_k,z_{k+1},\ldots,z_L\}, \end{aligned} \tag{1}$$

where M,N,L are the numbers of points on each dimensions, respectively. The function $f(x,y,z)$ is defined in a cubic volume ($x_1 < x < x_M, y_1 < y < y_N, z_1 < z < z_L$). The entire volume is sliced into many small cubes by the structured grid Eq.(1). For each cube, the tri-cubic spline interpolation evaluates the function as

$$f(\tilde{x},\tilde{y},\tilde{z}) = \sum_{m,n,l=0}^{3} c_{mnl}\tilde{x}^m\tilde{y}^n\tilde{z}^l \quad (0\le\tilde{x}<1, 0\le\tilde{y}<1, 0\le\tilde{z}<1) \tag{2}$$

where the rescaled variables are $\tilde{x} = (x-x_i)/(x_{i+1}-x_i)$, $\tilde{y} = (y-y_j)/(y_{j+1}-y_j)$, $\tilde{z} = (z-z_k)/(z_{k+1}-z_k)$, and the coefficients c_{mnl} are uniquely determined by the function values and its derivatives,

$$\{f, \frac{\partial f}{\partial\tilde{x}}, \frac{\partial f}{\partial\tilde{y}}, \frac{\partial f}{\partial\tilde{z}}, \frac{\partial^2 f}{\partial\tilde{x}\partial\tilde{y}}, \frac{\partial^2 f}{\partial\tilde{x}\partial\tilde{z}}, \frac{\partial^2 f}{\partial\tilde{y}\partial\tilde{z}}, \frac{\partial^3 f}{\partial\tilde{x}\partial\tilde{y}\partial\tilde{z}}\}, \tag{3}$$

evaluated at the eight corners of the cube, $(\{x_i,y_j,z_k\},\ldots,\{x_{i+1},y_{j+1},z_{k+1}\})$. The coefficients c_{mnl} can be represented by a vector $\mathbf{c}$, and the function values and its derivatives in Eq.(3) can also form a vector $\mathbf{b}$. These two vectors are connected by a universal constant 64×64 matrix $\mathbf{B}$:

$$\mathbf{Bc} = \mathbf{b}. \tag{4}$$

The interpolated function and its first-order derivatives are continuous over the entire volume ($x_1 < x < x_M, y_1 < y < y_N, z_1 < z < z_L$). In our case, this means the energies and the forces are continuous throughout the entire coordinate space, which is sufficient for simulating dynamics. Moreover, rather than interpolating the potential energies on-the-fly, we calculate and store the coefficients c_{mnl} for the entire surfaces before any trajectory calculations. By sacrificing the memory space, we achieved excellent time efficiency: the simulation of one PD-CE trajectory that propagates for 2 ps takes about 0.5 second on a single-core processor.

Figure S1 shows two representative potential curves of the interpolation and the corresponding derivatives of the 7th and the 9th adiabatic states of the neutral CH_3I molecule, which are the relevant states in our excited-state dynamics simulation. At $\theta = 0^\circ$, these two states are energy degenerate with the $^3Q_0$ and $^1Q_1$ diabatic states, and form a conical intersection at $R \approx 2.4$Å. At a larger bending angle, these two adiabatic states form an avoided

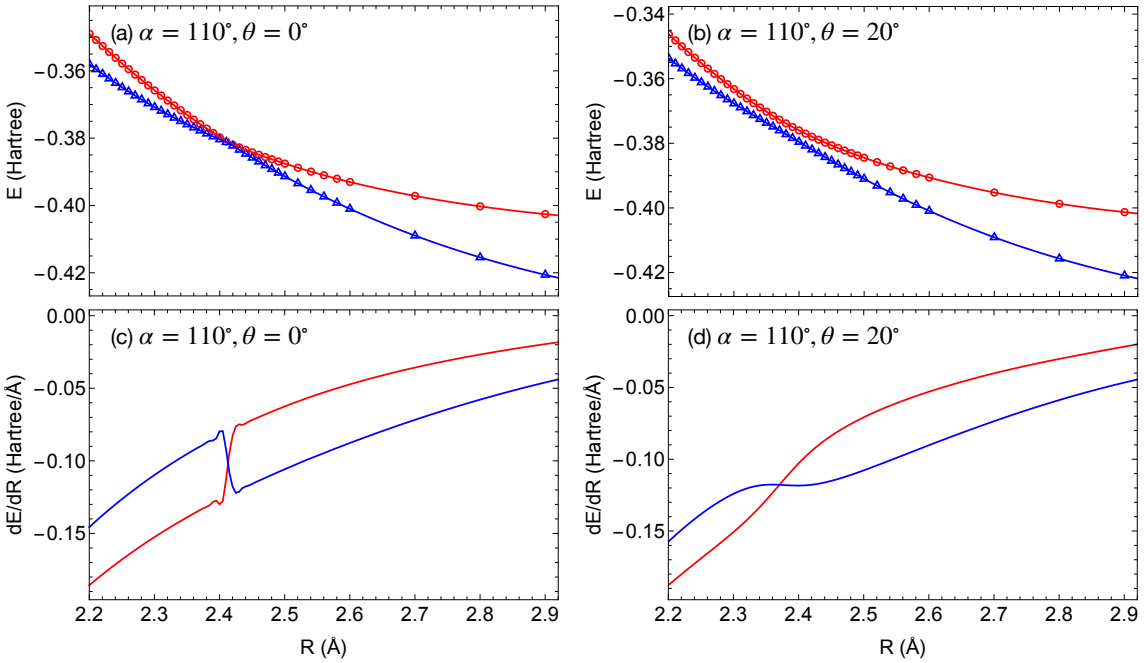

Fig. S1. Demonstration of the interpolated potential energy surfaces of the neutral CH_3I molecule. (a)-(b) The potential energies of the 7th (blue) and 9th (red) adiabatic states as a function of the C-I distance R at $(\alpha = 110°, \theta = 0°)$ and $(\alpha = 110°, \theta = 20°)$, respectively. The open markers denote the original eigen energies from the *ab initio* electronic structure calculations. The curves denote the interpolated potential functions. (c)-(d) The corresponding energy derivatives of the interpolated potential functions with respect to R.

crossing feature. The *ab initio* energies are smooth and accurate, which results in an interpolated potential function with high fidelity for both energies and forces.

The CH_3I^{2+} cation potential energy surfaces are extrapolated to characterize the Coulomb interaction and the charge-dipole interaction between the CH_3^+ and I^+ fragments, which can be written as

$$V_{CH_3I^{2+}} \approx V_{CH_3^+} + V_{I^+} + \left(\frac{1}{R} - \frac{C_4}{R^4}\right) \qquad (R > R_c^{ion}), \tag{5}$$

where $V_{CH_3^+}$ and V_{I^+} denote the internal energies of the CH_3^+ and I^+ fragments, and $R_c^{ion} = 10$Å is the cut-off distance in our calculation. The $V_{CH_3^+}$ component is approximated by averaging the potential energy of CH_3I^{2+} over $-60° \leqslant \theta \leqslant 60°$ at the cut-off distance, that is,

$$V_{CH_3^+} \approx \frac{1}{120°} \int_{-60°}^{60°} V_{CH_3I^{2+}}(R = R_c^{ion}, \alpha, \theta) d\theta. \tag{6}$$

Figure S2(a) shows the internal energy of CH_3^+ obtained from Eq. (6) compared with the *ab initio* energies from electronic structure calculations. We observe that the energy is nearly independent of the bending angle θ, and is almost symmetric about $\alpha = 90°$. These features indicate the internal energies of the CH_3^+ and I^+ fragments are separable when $R > 10$Å, making Eq. (5) a valid approximation.

The threshold energy V_{I^+} and the C_4 coefficient are obtained using least square fitting of $V_{CH_3I^{2+}} - V_{CH_3^+} - 1/R$ using ab initio energy points in the region $7\text{Å} \leqslant R \leqslant 10\text{Å}$, which results in a root mean square error of 0.00012 Hartree (0.003 eV).

Figure S2(b) shows the fit result of $V_{I^+} - C_4/R^4$ along with the *ab initio* energy points of $V_{CH_3I^{2+}} - V_{CH_3^+} - 1/R$. Although the extrapolation is not analytic, the discontinuity on the potential and its derivatives are sufficiently small, which has negligible influence on the simulated observables.

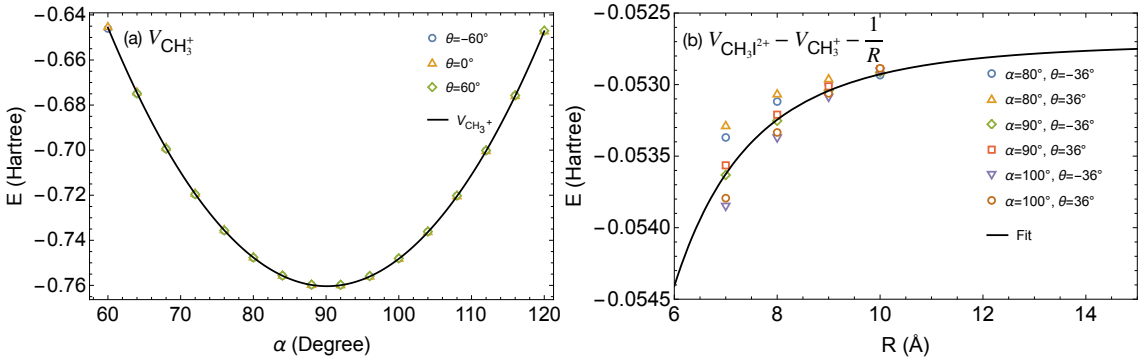

Fig. S2. Demonstration of the extrapolated potential energies of the lowest CH_3I^{2+} ionic state corresponding to the $I^+(^3P_2)$ threshold. (a) The energy of the CH_3^+ component as a function of α with $R = 10$Å. Black curve: the averaged energy according to Eq. (6). Open markers: energies obtained from *ab initio* calculations. (b) The extrapolated potential energy as a function of R. Black curve: The $V_{I^+} - C_4/R^4$ term of the potential energy obtained from the least square fitting. Open markers: energies obtained from *ab initio* calculations. Note only a small portion of the *ab initio* energy points used for averaging (fitting) are shown in (a) and (b).

2. Code availability

The code for the potential energy function and the *ab initio* potential energy data of CH_3I and CH_3I^{2+} used in this work are available upon request.

References

1. F. Lekien and J. Marsden. Tricubic interpolation in three dimensions. *International Journal for Numerical Methods in Engineering*, 63(3):455–471, 2005.